# The world ocean wave fields discerned from ERA-Interim spectra

Jesús Portilla-Yandún
Research Center of Mathematical Modelling (MODEMAT)
Escuela Politécnica Nacional, Quito, Ecuador

## Abstract

Ocean waves at any particular location are the result of the superposition of locally generated waves by wind, plus swells advected from somewhere else. Swells in particular can travel very long distances with marginal energy loss such that their signal, albeit reduced by dispersion, can be detected all across the oceans. Although our current approach for wave modeling and description has the wave spectrum as standard variable, most wave characterization methods are based on simplified integral parameters (e.g., $H_s$, $T_m$, $\theta_m$). These are indicative of the overall magnitude, but loose all the information stored in the spectral structure. Therefore, total wave fields derived from integral parameters are smooth and continuous while in reality wave fields have well defined spatial domains, they overlap one another, and they vary significantly along the seasons in response to the ever changing meteorological forcing. Using spectral partitioning techniques and the global spectral wave climate atlas GLOSWAC, the main wave fields active in the different ocean basins can be elucidated and separated from the integrated one. As the memory of the sea surface (waves) is longer than that of the atmosphere, these individual wave fields constitute a valuable new source of environmental information, and its characterization opens the way to more advanced wave analysis methods.

## Plain Language Summary

The present development constitutes a further processing level of global wave spectra, initiated (and based on) the point spectral characterization presented in GLOSWAC. This results in the disaggregation of the world ocean wave fields and its consequent characterization. To this end, a new clustering technique has been developed, based on spectral correlations among long-term wave systems, which prove strong for the purpose. Important advantages of these wave fields, are the specificity, compared to overall wave parameters, and the longer memory compared to wind. This constitutes a new source of environmental information and opens the door for several specific analysis and applications.

## INTRODUCTION

Waves are the product of surface winds transferring energy to the ocean in the form of momentum. However, differently than winds which change rapidly over spans of hours, or occasionally days, waves carry on that signal easily for days and even weeks (e.g., Barber and Ursell, 1948; Munk et al, 1963). This automatically means that the memory of the sea surface is much longer than that of the atmosphere. In turn, such a better memory implies also a wider spatial coverage as swells propagate and disperse across the oceans with marginal energy dissipation (Snodgrass et al., 1966). For instance swells generated by the northern and southern extra tropical storms can be detected (and impact regions) half a globe away (e.g., MacAyeal et al., 2006). In this regard, another disadvantage of wind fields, as information source, compared to waves, is that they cannot overlap in space, a stronger wind simply takes over the place of a decaying one (mass transport). In contrast, water as a transport medium allows for the occurrence of superimposing waves (energy transport) with different frequencies and traveling in multiple directions. In that context, the current state of the art for wave description constitutes another major advantage (e.g., Pierson and Marks, 1952). At the core of such description is the 2D wave spectrum, which at every single location represents the wave energy distribution in frequency and direction (e.g., Kuik et al., 1988; Donelan et al., 1996). Thanks to this representation, a sea surface perturbation propagating along a given direction can be traced from origin to destination, since waves travel rather independently from one another, particularly when they classify as swells.

Therefore, having spectral information at global scale, with records spanning over decades, is just too valuable a source of environmental information to be overlooked. This is the main motivation for the present study. Fairly recently the ECMWF made public the spectral data of the ERAI archive (Dee et al., 2011), which constitutes the first massive and consistent data set of this kind. During the last decades we have experienced the conception, implementation, development, and consolidation (through extensive verification) of wave models to reach their current state, the so called third generation models (e.g., Komen et al, 1994), which among other characteristics, implies the evolution and propagation of the spectral components, free from parametric empirical relationships (e.g., Hasselmann and Hasselmann, 1985; Cavaleri et al., 2007). This advance is crucial, as we now have access to the details of the energy distribution, instead of its resulting integral parameters (e.g., $H_s$, $T_m$, $\theta_m$), which may be easier to grasp and measure, but are much less rich in information (Holthuijsen, 2007). Indeed, global $H_s$ wave fields exist from models and even from satellite observations since long ago (e.g., Young and Holland, 1996), but elucidating the specific details of the many overlapping wave fields from that information alone is very hard, if not impossible. As it

will soon be illustrated, the magnitude of some wave fields is sometimes too feeble to be appreciated under the shadow of other stronger fields. To discern that information we can only rely on the wave spectrum.

The present work is a sequel of previous developments. Particularly the wave spectral characterization of the ERAI data set allowed the creation of a global atlas (GLOSWAC), which is the basis for this development (Portilla-Yandun, 2018). The available information in GLOSWAC is point specific, but from the several indicators in there, the spatial coherence of the different wave systems (or families) is pretty evident. The spatial concatenation of the local information results in the identification and consequently allows the extraction of the different wave fields. Such operation requires a dedicated methodology, which is the main subject of this paper, and is reported in detail in Section 2. From there on, as individual wave fields start to emerge from the grand total, the possibilities for environmental analysis (among others applications) arise accordingly. This is illustrated in Section 3 through compact examples, conveniently focusing on a secondary wave field (secondary in magnitude), belonging to the trade winds. This field is typically shadowed under other stronger fields, so by its extraction we expose it for any specific and individual analysis. The full characterization of each wave field is evidently beyond the scope of the present work, but the analysis of this field is deepened to certain extent to illustrate the potential of this technique and this new source of information.

It is probably worth mentioning that several approaches have been tried within this work to reach the objective, some were either unsuccessful or only partially successful, so they are not reported here. This emphasize the skills of the spectral correlations between wave systems, which is the path finally taken. Most relevant patters reveal themselves at once in global maps of this parameter, but some post-processing is needed to remove inconsistencies. This is discussed in some detail in Section 4, where results of the Self Organizing Maps technique are reported, showing that other processing possibilities may exist for wave spectra, which is the variable playing the central role. Finally, some immediate applications, that cannot be developed within the extent of the present paper, are hinted for further development.

## 2. METHODOLOGY

### *2.1.- Wave spectra from ERA-Interim*

The ERA-Interim (ERAI) from the *European Centre for Medium-Range Weather Forecasts* (ECMWF) is a re-analysis project that contains a wealth amount of atmospheric and oceanic

parameters (Dee et al., 2011), among them the ocean wave spectra computed from the WAM model (Hasselmann et al., 1988; Bidlot, 2012), which is the central variable for this study. The data set used here covers the period from 1979 to 2015 at 6 h interval output, making a total of 54,056 spectra per grid point. ERAI uses a spatial Gaussian grid with variable resolution whose lowest range, at the equator, is of about 110 km (Berrisford et al., 2011). This makes a total of 27,948 ocean grid points. The spectral grid is discretized in 30 frequencies from 0.035 to 0.55 Hz (1.1 geometric progression) and 24 directions. ERAI is the first archive to store long series of global wave spectra, superseded at present by ERA5 from the same center (Hersbach et al., 2020). The reason for using ERAI here instead of ERA5 is that the present work builds up on previous developments based on ERAI, not yet available for ERA5. Nevertheless, at global scale the resolution of ERAI is sufficiently good to elucidate the most important ocean patterns, and the upgrade of the present results to ERA5 data is not discarded for future developments.

### *2.2.- Wave spectral partitioning*

The spectral energy bins, although independently computed by the model, cluster themselves naturally conforming 3D surfaces that resemble topographic features. Physically each of these features is associated to a wave event generated by a particular and individual meteorological forcing (e.g., Ardhuin et al., 2019). Spectral partitioning consists in identifying those 3D features of the energy distribution. The scheme used here is that described in Portilla et al. (2009), which has been extensively applied to all types of data.

### *2.3.- Long-term spectral wave systems*

Long series of spectral data need to be characterized statistically, ideally preserving their spectral structure instead of reducing them to integral parameters (e.g., $H_s$, $T_m$, $\theta_m$). To this end, an ad hoc clustering method was developed by Portilla-Yandun et al., (2015). This method consists of collecting specific parameters of the spectral partitions (e.g., $T_p$, $\theta_p$) to obtain their empirical occurrence distribution in the native spectral grid. This distribution allows elucidating the wave families (or so called long-term wave systems) present at the reference location. Based on this method, the ERAI data set has been processed to develop a global spectral wave climate atlas (GLOSWAC). Those developments are reported in Portilla-Yandun, (2018), and publicly available at https://modemat.epn.edu.ec/nereo/.

### *2.4.- Wave spectral correlations*

By exploring point by point the wave families and their attributes (e.g., via GLOSWAC), their differential variations in space become evident. In this way, the spatial domain of a given wave system can be determined from multiple point source data in order to obtain coherent and separated spatial wave fields. A skillful parameter to distinguish the nuances of such connections is the coefficient of determination, computed as specified in equation 1. This scheme has been introduced for similar purposes in Portilla-Yandun and Cavaleri, (2016).

$$R_{i,j}^2 = 1 - \frac{\iint_{\theta f} \left[ E_i^m - E_j^n \right]^2 df d\theta}{\iint_{\theta f} \left[ E_i^m - \overline{E_i^m} \right]^2 df d\theta} \qquad (1)$$

In equation 1, *i* indicates the reference geographical point, while *j* refers to any remote point on the spatial grid. In turn, *m,n* represent any wave family at those locations respectively, and *E* is the time series of the partial (partition) spectra for the whole period (37 years). Note that this is a standard $R^2$ parameter adapted to the wave spectrum, so it can also take negative values.

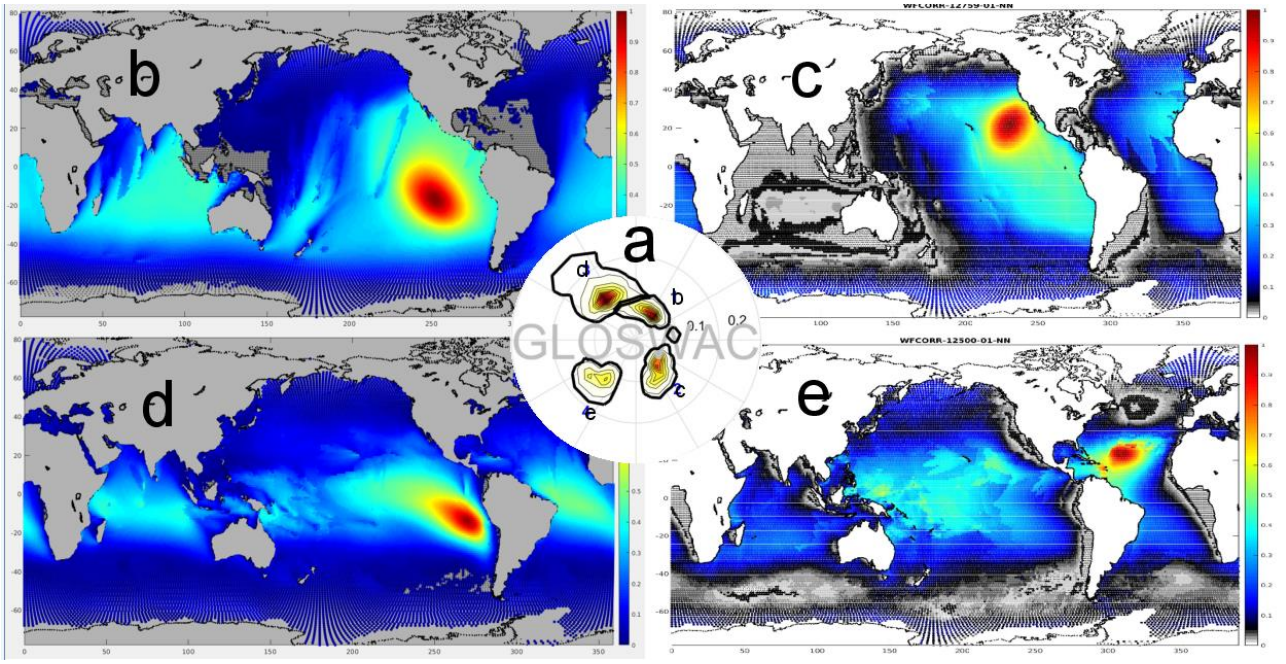


Figure 1. Spectral wave correlations among wave systems a) central panel, long-term wave systems at 0ºN-105ºW, colors indicate recurrence, b) extratropical southerly waves (Antarctic), c) extratropical northerly waves, d) southern trade-wind systems, e) northern trade-wind systems.

Figure 1, shows the $R^2$ structures of some of the dominant wave systems on earth. The central panel shows the spectral statistics matrix (wave families), of a point over the equator (0º latitude, 105ºW) that conveniently depicts only the four exemplified systems. This constitutes the departing information to compute correlations. The *m*, *n* nomenclatures in equation 1, refer to each of these families. In each of the map panels the reference point (*i*) corresponds to the highest correlation value. Panel 1b shows the dominant wave field in the oceans, the southern swells. As storms transit freely around Antarctica they constantly generate swells that are then radiated over almost the entire globe (e.g., Derkani et al., 2021). The Caribbean and the Philippine seas, apart from enclosed seas, appear to be the only shadow areas. However, skillful as they prove, it is clear that correlations are not filtering out certain details, as conspicuously some regions of the Caribbean, and the east coast of the U.S., for instance, display positive correlation values, while there is no possibility for the southern swells to reach those areas. The reason is that for some points and wave systems the correlations as such may be to some extent spurious, at least at lower values and for the purpose intended here. Some wave systems (e.g., U.S. east coast) may be active with similar seasonality and similar spectral characteristics (e.g, $T_m$, $\theta_m$) as the southern swells, hence they appear correlated, although they do not belong together as wave systems. Tackling this issue is the subject of the next section. Apart from that, note that those "spurious" correlations open the door for other type of analyses as they may point out to climate correlations, the so called tele-connections (e.g., Nigam, 2003). This is discussed further in section 3.3.

In turn, panels 1c, 1d, and 1e show the structures of the northerly swells, and the southern and northern trade-wind fields respectively, from which some interesting features are worth mentioning. For instance, it is striking to see that differently from the southern storms, the northern ones do not have an associated component in the Indian Ocean. Nevertheless, its large extent encompasses the Pacific and Atlantic Oceans. Turning to the southern trade-winds, note that although the reference point, in this example, is located in the eastern Pacific, strong correlations appear also in the Atlantic, Indian, and western Pacific Oceans, showing that related features exist in those basins as well, as we know from the wind fields (e.g., Hadley, 1735; Maury, 1855; Ferrel, 1856; Persson, 2006). The structure of the northern trade-winds field is also very complex, with a clear pattern in the Atlantic, but developing several jet regions all over the Pacific. Its correlations in the Indian Ocean appear again feeble, but conversely it also appears to be correlated with the southern trades both in the Atlantic and the Pacific Oceans. As mentioned earlier, elucidating all these complexities requires complementary processing, which is the subject of the following sections.

### *2.5 Spatial consistency of the wave systems*

The use of correlations proves skillful but not sufficient on its own as a mechanism to neatly discern the spatial-spectral structures, so we have to either resort to the use of another clustering technique, or introduce a complementary post-processing routine (or both). For the former, the Self Organizing Maps technique (SOM, Kohonen, 2001; Vesanto et al., 2000) has been tested, showing interesting skills but similar shortcomings. These results and its perspectives are reported in Section 4.1, while it becomes clear that either post-processing or the use of complementary steps is the way to go. Keeping correlations at the core of the process we observe that at higher or intermediate values, these structures are not spurious but indeed identify the target wave field. In addition, a particular wave field can be "observed" from different reference points, so if the same wave field is discerned at relatively high correlation thresholds but from a sufficient number of locations, it is then possible to generate the necessary redundancies to consolidate its actual extent. In this way, the resulting field is obtained as the union of the several local sub-fields, as:

$$S = \bigcup_{k=1}^{K} S_{k,t} \qquad (2)$$

where $S$ is the consolidated wave field, while $S_{k,t}$ represents the sub-fields corresponding to the reference point $k$, trimmed at threshold $t$, being $K$ the total number of reference points. Under this setup, thresholding is aimed to remove spurious correlations, while a large number of reference points ($K$) helps to consolidate the entire field, these two parameters are therefore related. For a specific field, the higher the threshold, the higher the number of sub-fields required. Ideally, these mutual correlations should be computed for every grid point against each other, but this operation is computationally expensive so it has to be kept within limits. In the present development, a range of $K$ between 20 and 50 has been used, with thresholds ranging from 10 to 40%. These settings are readily verified from the consistency of the wave field's parameters (e.g., $H_s$, $T_m$, $\theta_m$), which are not part of the computation. Those results are presented later on in section 3.

Using the southern trade-winds field as illustrative example, Figure 2 shows four of its sub-fields. Note that although the reference points are in different ocean basins, the global features displayed are always similar. Particularly those from the eastern Pacific, the Atlantic, and the Indian Oceans are very smooth and regular, with similar characteristics. They all start narrowly localized at the west side of the continental borders, at about 35ºS, to then fan out north-westwards over their oceans (e.g., Wyrtki and Meyers, 1976). In turn, the corresponding trades in the central Pacific show more complexity, with a less defined starting point arguably because there is no land mass for

a fixed reference. Moreover, its fanning out over the Polynesian and Melanesian islands is severely hindered and therefore more irregular.

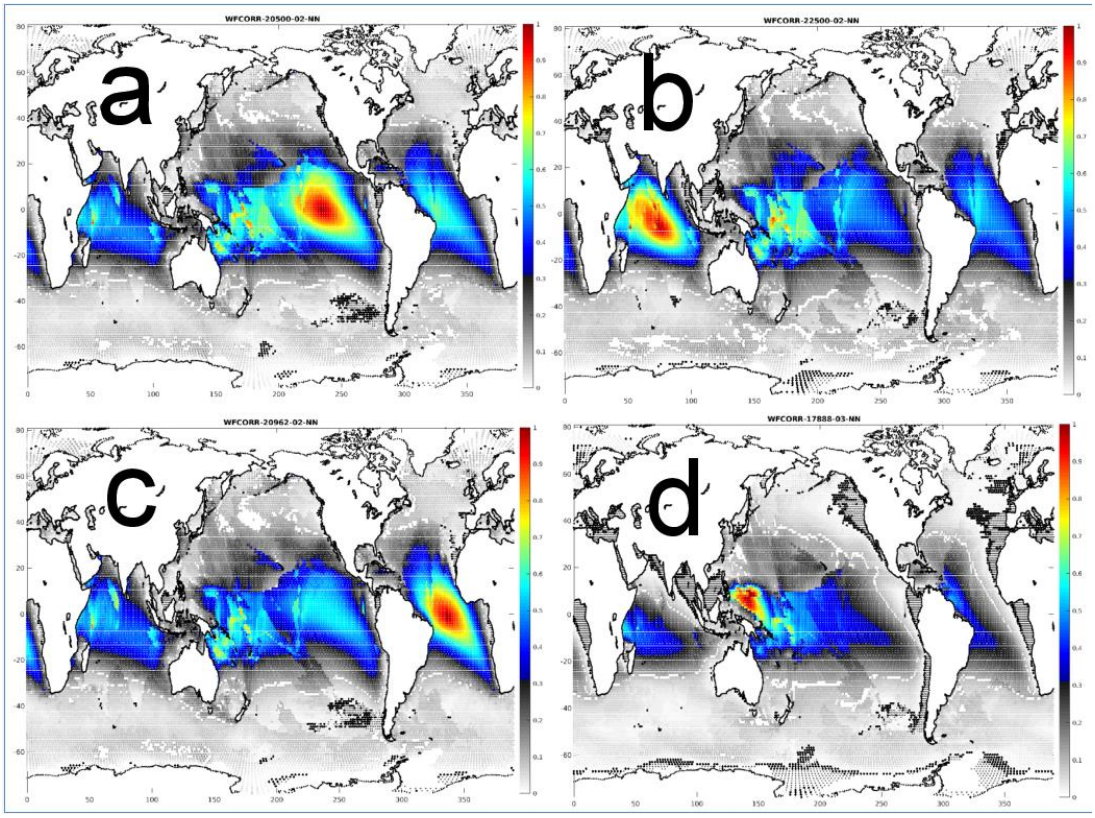


Figure 2. The southern trade winds "observed" from different oceans basins, corresponding to the points with the highest correlation in each panel. Rainbow colors indicate correlations above 0.3 (as possible trimming threshold), whereas lower values are shown in gray scale.

### *2.6 Sequential extraction*

The present processing scheme, and also the concepts of spectral partitioning and spectral statistics, are not purely numerical, but a combination of numeric and physically assisted algorithms. By interventions like the steps introduced in the previous and in this section, the system is constrained (or helped) to follow a specific course based on the underling physics, otherwise the computational burden would be overwhelming even for modern computers. In addition, an unconstrained scheme will hardly converge to the desired output, as several clustering solutions are possible from the available data. In this regard, the strategy of sequential extraction of the wave fields constitutes another intervention. The generating wind fields cannot overlap with each other, but their corresponding wave fields do have this possibility, superimposing one another like onion layers. Some fields, specially those with larger coverage and magnitudes, are easier to detect and extract, while the weaker and more local fields are more challenging. The extraction therefore is not

random, but organized according to the facility to identify a certain field, which basically means its relative magnitude.

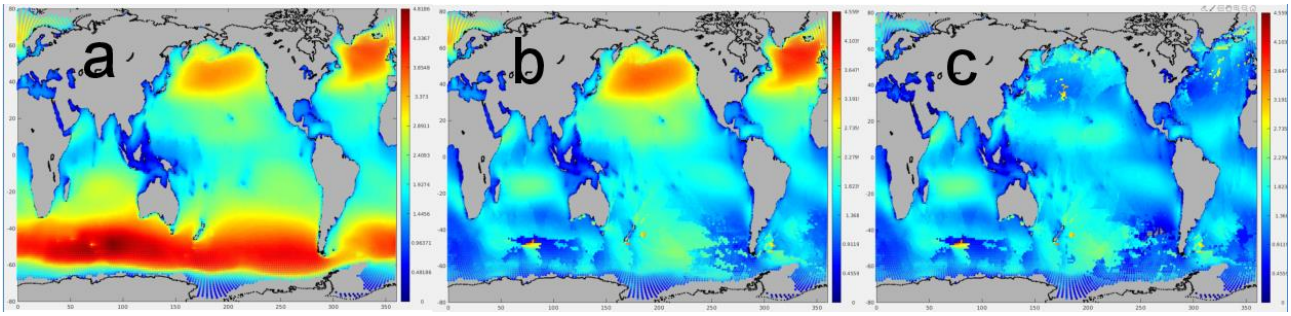


Figure 3. Average $H_s$ wave fields illustrating the sequential extraction. a) total, b) after extracting the southern storm swells, c) after further extracting the northern storm swells.

This idea is illustrated in Figure 3, where panel 3a shows the total average $H_s$ over the study period, a rather familiar picture of the global wave field, often available in text books (e.g., Cruz, 2010). As observed before (in Figure 1), the southern storms and its associated swells constitute a dominant and clearly discernible feature, hence they are easy to detect and extract, as shown in panel 3b, where clearly a significant fraction of the total energy is now missing. The next dominant feature corresponds to the northern storms and its associated swells. It is worth mentioning that this field is by far more complex and fragmentary than the previous one, likely due to the continental land configuration of the north hemisphere (e.g., Marshall and Plumb, 2007). In any case, once extracted another less familiar but interesting picture emerges (panel 3c). Particularly the trade-wind fields (from both hemispheres) start to reveal, apart from other conspicuous local features and jets. Note that the magnitude of the underlying layer (in $H_s$ terms) is less than half that of the extra-tropical storms. Finally, following this process, it is possible to extract, one at the time, all the existing wave fields, which accounting for the individual components in the different basins, they are in the order of a hundred. The potential of the individual fields for environmental analysis is developed in the next section.

## 3. RESULTS

### *3.1 Wave fields characterization and verification of self-consistency*

No matter how much we complain about integral parameters losing spectral information, these remain the best as wave descriptors, as they provide useful practical magnitudes, particularly when they refer to individual wave systems. Therefore, the obtained wave fields are presented and

analyzed here in the light of these magnitudes (e.g., $H_s$, $T_m$, $\theta_m$). For the specific case examined in section 2.5 (the southern trades), once extracted, Figure 4 shows their corresponding average characteristics.

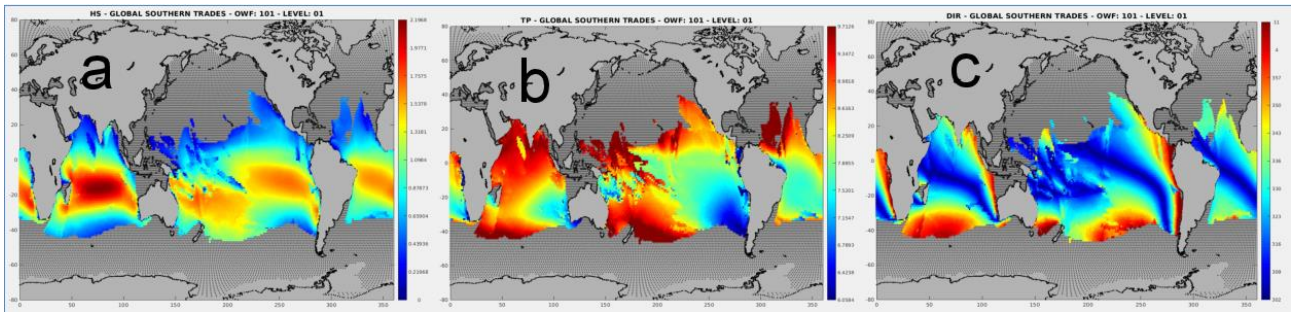


Figure 4. Average characteristics of the wave field corresponding to the southern trade winds. a) Wave height, b) mean period, c) and mean direction.

Similarly as for the correlation structures, in Figure 4 we observe coherent shapes of the main parameters, and also related patterns in the different ocean basins. This statement might seem trivial at first glance but is not quite so because all these parameters (i.e., $R^2$, $H_s$, $T_m$, and $\theta_m$) are highly independent from each other, so the main reason for their smoothness and continuity is that indeed they belong to the same wave field. Nevertheless, we do observe irregularities, but these are mainly associated to the presence of obstructions. This is particularly the case of the central Pacific component, which apart from not having a continental land mass reference at the origin (as the other three do), it is hindered by many islands, as mentioned earlier. The Indian Ocean component is remarkable for its higher $H_s$ magnitude, which accordingly derives in higher $T_m$ values. The directional patterns are interesting in their similar behavior in the three basins, the core band (in dark blue) encompasses the more oblique directions (NW) and its extent seems to bend at lower latitudes. As waves are not significantly affected by the Coriolis effect (e.g., Backus, 1962), this bending must come from the wind field itself. In turn, the bands closer to the continents, as well as the south boundaries, exhibit more marked northward directions. Although there is much more to analyze from Figure 4, the objective here is not to describe any particular wave field in detail (a task worth in itself a dedicated study), but to illustrate the methodology and its applicability, for which the southern trades constitute an interesting example.

### *3.2 Time variability of the wave fields*

Having the wave field extracted from the rest of layers, many of its characteristics can be readily established. Among them, the time variability is particularly interesting in the climate context.

Figure 5 shows the seasonal variability of the southern trades wave field. As expected, we observe the larger magnitudes associated to the JJA period, and the lower to DJF (e.g., Wyrtki and Meyers, 1976). Other features are also interesting, as the shape and extent of the field domains. We observe for instance the field's core in the Atlantic extending further north-westwards during the JJA and SOM season, covering the north of Brazil. Note that these atmospheric features are responsible for the transport of humidity from higher to lower wind magnitude areas, hence affecting directly the weather on different regions, and eventually been altered by other global anomalies (e.g., Caviedes, 1973; Chung, 1982). Apart from the natural differences among the seasons we observe that the range of variation is not particularly large. On the contrary, note that this system is prevalent in the southern oceans all along the year. In terms of the overall mean and global $H_s$ (a very bulky parameter) the range of variation is from 1.85 m in SON to 1.92 m in MAM. However, the time evolution of the wave field involves not only the total amount of energy delivered by the atmosphere, but mainly other parameters as the spatial distribution of that energy (e.g., Barnett, 1977).

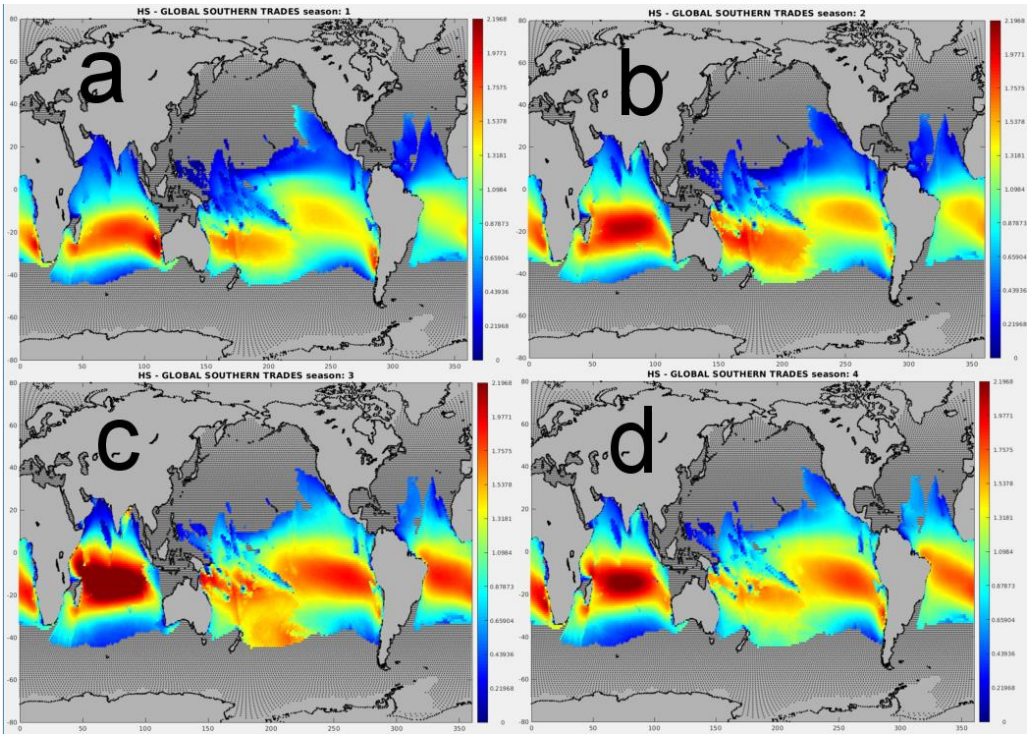


Figure 5. Seasonal variability of the southern trades wave field a) DJF, b) MAM, c) JJA, d) SON

It has been argued for instance that the position of the ITCZ advances abnormally into the south hemisphere during ENSO years (e.g., Pazan and Meyers, 1982; Donguy and Henin, 1980), while in turn the trades in the central Pacific intensifies (e.g., Reiter, 1978). These apparently contradictory effects suggests a significant zonal variation of the southern trades (e.g., Philander, 1983).

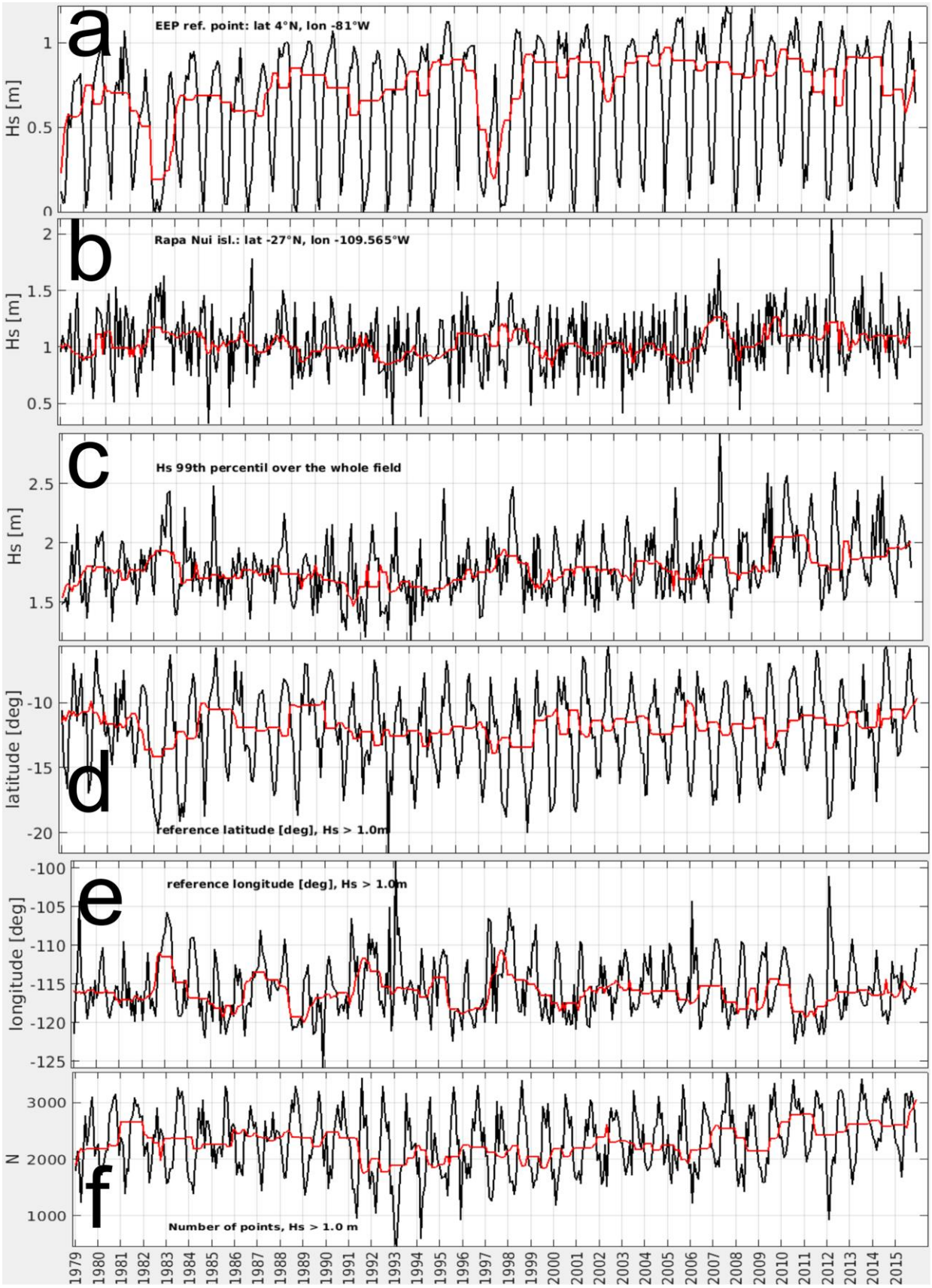


Figure 6. Inter annual variability of the eastern Pacific component of the southern trades. a) monthly mean $H_s$ at 4°N, 81°W. b) monthly mean $H_s$ at Eastern island. c) monthly $H_s$ 99th percentile of the whole field. d) average latitude of the points with $H_s$ > 1.0 m. e) same as (d) for longitude. f) Number of points with $H_s$ > 1.0 m. The red series correspond to the moving median.

Similar maps as those in Figure 5, but on month-yearly basis (not shown) depict indeed a large space-time variability. However, to make sense of the overwhelming amount of maps, we need to resort to time series as presented in Figure 6. To simplify the analysis in this section we refer only to the eastern Pacific (EP) component of this field. In panel 6a, a point on the north east border (4°N, 81°W) shows a nicely modulated $H_s$ signal, that unequivocally follows the seasons. In addition, we observe two conspicuous lows in 1982-83, and 1997-98, which correspond namely the two notorious ENSO events (NEE) within the period. These characteristics led to Portilla-Yandun et al., (2016), to identify that region as indicative for ENSO. This particular behavior however, is not reproduced at other locations. At Eastern island for instance (Rapa Nui, 27°S, 109.5°W), the seasonality is not at all obvious, nor are the lows during the NEE. On the contrary, there is a slight $H_s$ increase in those years with otherwise an erratic signal, albeit rather uniform on the median. Panel 6c shows the 99th percentile (a more stable parameter for the maximum) computed over the entire EP component. This too shows a slight increase during the NEE years, instead of the opposite, in agreement with the premise of its intensification, and revealing the complex structure of the field and its variations. To gain insight of the spatial displacement of this wave field, panels d, and e, show respectively the average latitude and longitude of the points above a given threshold ($H_s$ > 1.0 m). The seasonal modulation is more evident in the latitude displacement, while longitude seems to be modulated in yearly spans. During the NEE years, the core moves slightly southwards, and more prominently eastwards. However, this occurs in other years as well, and therefore it is not a strong attribute of ENSO.

Finally, and from another perspective, panel 6f shows the number of points above the selected threshold (out of 4600 for the total EP component). This parameter is related to the total area affected by intense winds, indicating hence eventual weakening or intensification. Apart from the good seasonal modulation, and a relative high in 1981, we observe an apparent steady increase of this parameter from 1991 onward, which in fact is also apparent in the 99th percentile. From the climate change perspective, this suggests a trend of enhanced EP southern trades, but a 25 years period is probably to short to draw firm conclusions in this regard, and not a direct objective of the present work. All these aspects are hinted here to illustrate the potential of this new source of information, and it is clear that there is a lot more to scrutinize. For instance, the parameters presented in Figure 6 correspond only to the EP component of the southern trades, while there is evidence that its southwards displacement causes a northward displacement of the Atlantic Ocean component to balance the global atmospheric pressure differences (Caviedes, 1973). Other conspicuous anomalies, as those visible in the years 1993, 2007, and 2012, beg for further analysis. However, these compelling details are beyond the scope of the present study and will be reserved

for further and specific studies. For the time being and the present purposes it is necessary to move on to other examples, which are developed in the next section.

### *3.3 Spatial relationships among wave fields (teleconnections)*

The earth is a whole and complex dynamic system in which the driving solar radiation varies daily and seasonally. The atmosphere buffers this signal, helped by the oceans which granted the large heat capacity of water buffers the signal even further, allowing life on earth, but making the physics of the whole system just too complex. Its responses are not linear and direct, but may take time to manifest, or emerge at remote locations. Indeed, systematic variations at one location have prove strongly correlated with variations in completely different places. These are the so called teleconnections, from which a good reference is that of the atmospheric pressure differences between Darwing (Australia) and Tahiti in the central Pacific, used in the Southern Oscillation Index (e.g., Trenberth, 1984). These connections are statistically born, and they are otherwise difficult to explain physically.

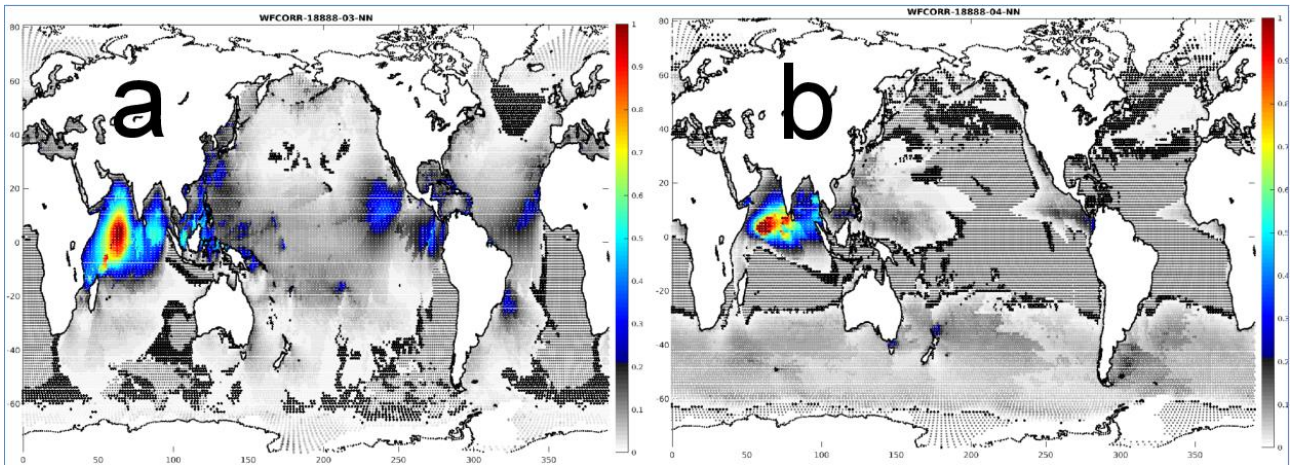


Figure 7. Spectral correlations of the Indian Ocean monsoons, a) winter, b) summer.

As seen from the beginning (in the southern swells), global correlations are ubiquitous in the wave fields. Among the many that can be elucidated from from these data, some interesting features include those of the Indian Ocean monsoons (Figure 7), by definition an inter-seasonal reversal of the local prevailing winds (e.g., Ramage, 1971; Hartmann, 2016). As seen in Figure 1, the Indian winter monsoon is uncorrelated to the northern storms, and only weekly correlated to the northern trades. It is therefore a more localized phenomenon. Indeed, a correlation map of this system shows low values in the global context (panel 7a), except for the surrounding regions in the Arabian sea, the Bengal bay, and some areas around Indonesia. Apart from these regions, interestingly enough,

we observe good correlation plumes in regions located almost half a globe away, namely the wind jets of Central America, plus other features in the region south west of Baja California, Salvador in Brazil, and Senegal in Africa (panel 7a), without further emphasizing the small regions around some Pacific islands.

The summer monsoon is also peculiar in the global context (panel 7b), as it looks uncorrelated to the large and dominating patterns, and therefore very distinct locally. Its correlation covers also the Arabian sea and Bengal bay, extending over the Philippine sea, albeit at lower magnitudes. Then again, its correlation to the westerlies in the EEP (near Panama) becomes noticeable, including also the similar feature in tropical Africa, covering the Gulf of Guinea. Do these correlations point out to physical whether relationships or are they spurious? Similar questions arise for the relationship between the summer monsoon and the southern extratropical areas, where also low but uniform correlations are depicted. Individual isolated wave fields are presented here as a new source of information, from which this sort of questions can potentially be answered, and although such information is somehow already contained in the driving wind signal, the persistence of its footprint on the water surface offers new and promising opportunities for environmental data analysis.

## 4. DISCUSSION AND PERSPECTIVES

Discerning and understanding the components of the wave fields of the different ocean basins is an exciting and fundamental task from the environmental point of view. Particularly because this signal is very clear, and provides new insights into some earth physical processes, otherwise difficult to distinguish from other data. The motivation and intention is not at all new, in fact all global wave characterization efforts point in this direction. However, the total wave height as working variable is already exhausted in this regard. A compelling approach is that of Alves, (2006) in which localized wave fields are used to synthetically generate its corresponding wave fields and analyze its characteristics (magnitude, persistence, among others). In the present work, historical records are used instead. In modern times where models already compute the wave spectrum, and several satellites observe it on a global and daily basis using state of the art technology, we should not set for less.

The several clustering schemes used here are numerically born, but they are physically and statistically assisted, this is necessary due to the volume and complexity of the data. The computations of section 2.4 are very demanding, even with these aids. For the grid resolution of the ERAI, a total of about 800 correlation points has been used, but higher resolution data (e.g. ERA5)

involves more details and hence requires more reference points. Therefore the computational capacity is a technicality that cannot be overlooked.

In the present study, the whole implementation is based on spectral partitioning, but pursuing the use of this technique it is not an aim. What is indeed pursued is the use the available spectral information. In previous studies (e.g., Portilla-Yandun et al., 2019) other techniques have been explored, i.e., SOM, for related purposes and with promising results. Section 4.1 reports the output of this technique in post-processing mode. When the main purpose is to elucidate the data patterns, any skillful method should be discarded.

The applicability of the obtained information is significant. This study has been oriented mainly to the most obvious, which is climate analysis, but other areas such as data assimilation, wave model evaluation at spectral level, renewable energy resources, among others, have a lot to benefit from the present results.

Finally, it is clear that the release of ERA5 has the potential to render ERAI obsolete. So the corresponding upgrade of the present results must be considered. In addition, similar results from observations would be just too desirable. Well equipped satellites have been measuring wave spectra for decades by now. Hopefully those data will make it to the global data mainstream soon.

### *4.1 Further processing with Self Organizing Maps (SOM)*

Dealing with complex and massive data proves often challenging. In this regard, all tools at hand should be put at work together, as some may have interesting skills to reach the objective. In this work, as complementary tool, the SOM technique has been used to post-process the wave fields. Figure 8 shows an example corresponding to the wind jets in Central America. The isthmus is mountainous but possesses three narrow passages at Tehuantepec, Papagayo, and Panama, where winds are funneled from the Caribbean to the Pacific (Chelton et al., 2000). These winds are very local but the consequent wave field extends over a relatively vast region in the Pacific Ocean. As can be seen in Figure 8a, the jets structure is complex, with directions all over the third quadrant (different flavors). There are components with marked north-south directions, but others occur perpendicularly, with also oblique directions from NW and NE. Moreover, as each of the passages generates its own wave field, these overlap over certain areas. With the use of SOM, many of these details can be further recognized. For the example in Figure 8, a number of 56 prototypes has been used, with otherwise default software parameters. Note however that the variable in use for SOM in this case are not directly the spectral time series, but the wave families matrices, obtained from the spectral characterization.

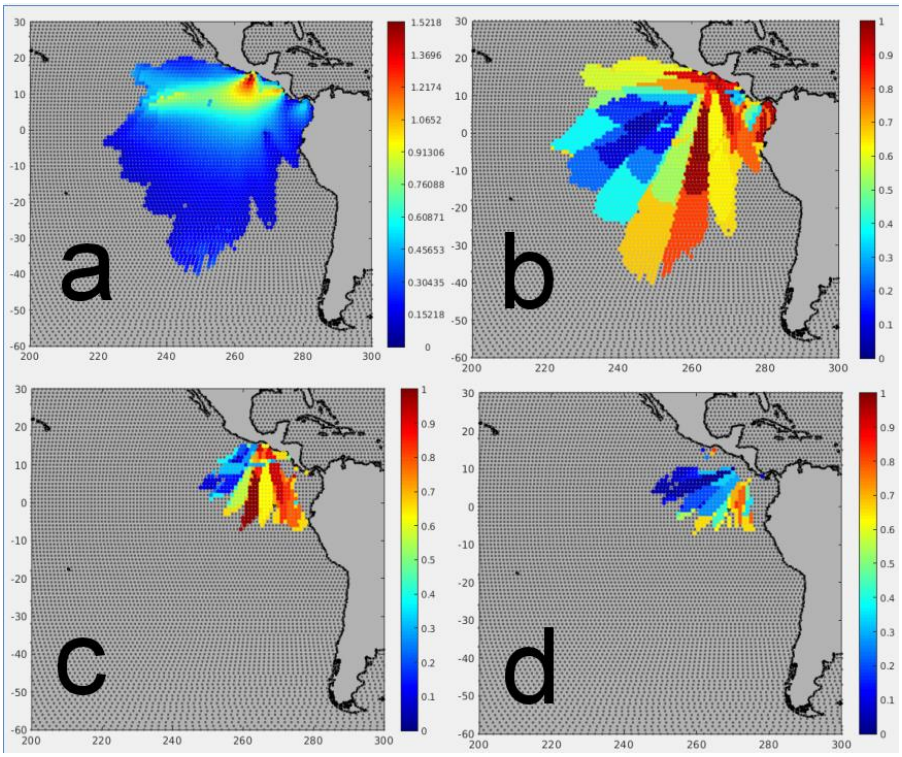


Figure 8. Wave field of the wind jets in Central America. a) average $H_s$, b, c, d, various sets of overlying prototypes obtained with SOM.

That is a post-processing role, as the amount of spectra, grid points, and wave families, makes an overwhelming amount of inputs for SOM, even for the small field of the Central America jets. In any case, it is interesting to see that different techniques provide consistent results, suggesting that these wave fields are characterized by strong attributes. Further on, the SOM clusters provide a good assessing tool for the specific analysis of the many components detected.

On a final note, the resolution of the data must also be commented. Indeed the spatial ERAI resolution is rather course, but in this example we observe that even for a localized wave field specific details are well captured. The reason again is the wave spectrum, since each grid point is further discretized in the spectral domain, acting thus as a local refinement, hence capturing the variations of the wind field.

## SUMMARY AND CONCLUSIONS

The present development constitutes a further processing level of global wave spectra, initiated (and based on) the point spectral characterization presented in GLOSWAC. This results in the disaggregation of the world ocean wave fields and its consequent characterization. To this end, a new clustering technique has been developed, based on spectral correlations among long-term wave

systems, which prove strong for the purpose. Important advantages of these wave fields, are the specificity, compared to overall wave parameters, and the longer memory compared to wind. This constitutes a new source of environmental information and opens the door for several specific analysis and applications.

## ACKNOWLEDGMENTS

This work was carried out in the framework of the project EPN-PIGR-1908. Wave spectra from ERAI was downloaded from the ECMWF (https://www.ecmwf.int/). Wave spectral statistical indicators are available at the GLOSWAC website (https://modemat.epn.edu.ec/nereo/)

## REFERENCES

Alves, J.H., 2006.Numerical modeling of ocean swell contributions to the global wind-wave climate. J. Ocean Modell. 11,98–122. http://dx.doi.org/10.1016/j.ocemod.2004.11.007.

Ardhuin F., Stopa J., Chapron B, Collard F, Husson R, Jensen RE, Johannessen J, Mouche A, Passaro M, Quartly GD, Swail V., and Young I., (2019), Observing Sea States. Front. Mar. Sci. 6:124. https://doi.org/10.3389/fmars.2019.00124

Backus G., (1962), The effect of the earth's rotation on the propagation of ocean waves over long distances, Deep Sea Research and Oceanographic Abstracts, V9, I5–6, 185-197, https://doi.org/10.1016/0011-7471(62)90168-7

Barber, N., Ursell F., (1948). The Generation and Propagation of Ocean Waves and Swell. I. Wave Periods and Velocities. Philosophical Transactions of the Royal Society A: Mathematical, Physical and Engineering Sciences, 240(824), 527–560. https://doi.org/10.1098/rsta.1948.0005

Barnett T., (1977). The Principal Time and Space Scales of the Pacific Trade Wind Fields, Journal of the Atmospheric Sciences, V34, I2, 221–236. https://doi.org/10.1175/1520-0469(1977)034%3C0221:TPTASS%3E2.0.CO;2

Berrisford P., Dee D., Poli P., Brugge R., Fielding M., Fuentes M., Kållberg P., Kobayashi, S., Uppala S., Simmons A., (2011), The ERA-Interim archive Version 2.0, ERA Report Series, https://www.ecmwf.int/node/8174

Bidlot, J., (2012). Present status of wave forecasting at ECMWF. In Proceeding from the ECMWF workshop on ocean waves (pp. 25-27). https://www.ecmwf.int/node/8234

Cavaleri,L.,Alves J., Ardhuin F., Babanin A., Banner M., et al., (2007), Wave modelling: the state of the art, Progress In Oceanography, 75(4), 603-674, 2007. https://doi.org/10.1016/j.pocean.2007.05.005

Chung, J.C. (1982), Correlations between the tropical Atlantic trade winds and precipitation in northeastern Brazil. J. Climatol., 2: 35-46. https://doi.org/10.1002/joc.3370020104

Caviedes, C., (1973). Secas and El Niño: two simultaneous climatical hazards in South America. *Proc Assoc Amer Geogr*, *5*, pp.44-49.

Chelton, D., Freilich M., and Esbensen S., (2000), Satellite observations of the wind jets off the Pacific coast of Central America, Part II: Regional relationships and dynamical considerations, Mon. Weather Rev., 128, 2019–2043, https://doi.org/10.1175/1520-0493(2000)128%3C1993:SOOTWJ%3E2.0.CO;2

Cruz J., (2010), Ocean wave energy, current status and future perspectives. Springer. ISBN 9783642094316, pp. 431.

Dee, D. P., Uppala, S. M., Simmons, A. J., Berrisford, P., Poli, P., Kobayashi, S., … Vitart, F. (2011). The ERA-Interim reanalysis: Configuration and performance of the data assimilation system. Quarterly Journal of the Royal Meteorological Society, 137(656), 553–597. https://doi.org/10.1002/qj.828

Derkani, M. H., Alberello, A., Nelli, F., Bennetts, L. G., Hessner, K. G., MacHutchon, K., Reichert, K., Aouf, L., Khan, S., and Toffoli, A.: (2021), Wind, waves, and surface currents in the Southern Ocean: observations from the Antarctic Circumnavigation Expedition, Earth Syst. Sci. Data, 13, 1189–1209. https://doi.org/10.5194/essd-13-1189-2021

Donelan M.., Drennan W., Magnusson A., (1996). Nonstationary Analysis of the Directional Properties of Propagating Waves. Journal of Physical Oceanography, 26(9), 1901–1914. https://doi.org/10.1175/1520-0485(1996)026%3C1901:NAOTDP%3E2.0.CO;2

Donguy J., Henin C., (1980). Surface conditions in the eastern equatorial Pacific related to the intertropical convergence zone of the winds. Deep Sea Research Part A. Oceanographic Research Papers, 27(9), 693–714. https://doi.org/10.1016/0198-0149(80)90023-0

Ferrel W., (1856). An essay on winds and the currents of the Ocean. Nashville Journ. Medicine Surgery, 11 : 287-230.

Hadley G., (1735). Concerning the Cause of the General Trade-Winds, Philosophical Transactions of the Royal Society of London, 39(436-444), 58–62. https://doi.org/10.1098/rstl.1735.0014

Hasselmann, S. and K. Hasselmann, (1985), Computation and parameterizations of the nonlinear energy transfer in a gravity-wave spectrum. Part I: a new method for efficient computations of the exact nonlinear transfer, Journal of Physical Oceanography, 15, 1369-1377, https://doi.org/10.1175/1520-0485(1985)015%3C1369:CAPOTN%3E2.0.CO;2

Hasselmann S., Hasselmann, K, Janssen P., et al. (1988). The WAM model - A third generation ocean wave prediction model. Journal of Physical Oceanography. 18 (12): 1775–1810, https://doi.org/10.1175/1520-0485(1988)018%3C1775:TWMTGO%3E2.0.CO;2

Hartmann D., (2016). Global Physical Climatology. Second Edition, 485 pp., Elsevier Science, ISBN: 978-0-12-328531-7. https://doi.org/10.1016/C2009-0-00030-0

Hersbach, H., Bell, B., Berrisford, P., Hirahara, S., Horányi, A., Muñoz-Sabater, J., … Thépaut, J. N. (2020). The ERA5 global reanalysis. *Quarterly Journal of the Royal Meteorological Society*, *146*(730), 1999–2049. https://doi.org/10.1002/qj.3803

Holthuijsen, L. (2007), Waves in oceanic and coastal waters, Cambridge University Press, 387 pp. ISBN: 9780511618536, https://doi.org/10.1017/CBO9780511618536

Kohonen, T., 2001. Self-Organizing Maps, vol. 30. Springer Series in Information Sciences. http://doi.org/10.1007/978-3-642-56927-2.

Komen G., Cavaleri L., Donelan M., Hasselmann K., and Janssen P., (1994), Dynamics and Modelling of Ocean Waves. Cambridge University Press, 532 pp. ISBN 0-521-47047-1

Kuik, A., van Vledder G, Holthuijsen L., (1988), A method for the routine analysis of pitch-and-roll buoy wave data, J. Phys. Oceanogr., 18, 1024–1034. https://doi.org/10.1175/1520-0485(1988)018%3C1020:AMFTRA%3E2.0.CO;2

MacAyeal, D., et al. (2006), Transoceanic wave propagation links iceberg calving margins of Antarctica with storms in tropics and Northern Hemisphere, Geophys. Res. Lett., 33, L17502, https://doi.org/10.1029/2006GL027235

Marshall J., Plumb A., (2007). Atmosphere, Ocean and Climate Dynamics, an introductory text. Elsevier Academic Press, 319 pp. ISBN: 9780125586917.

Maury M., (1855), The physical geography of the sea, Sampson & Co., London, pp. 318, https://doi.org/10.5962/bhl.title.102148

Munk W., Miller, G., Snodgrass, F., Barber, N., (1963). Directional Recording of Swell from Distant Storms. Philosophical Transactions of the Royal Society A: Mathematical, Physical and Engineering Sciences, 255(1062), 505–584. https://doi.org/10.1098/rsta.1963.0011

Nigam S., (2003), Teleconnections, Encyclopedia of Atmospheric Sciences, J. Holton (editor), Academic Press, 2243-2269, ISBN 9780122270901, https://doi.org/10.1016/B0-12-227090-8/00400-0

Pazan S., Meyers G., (1982). Interannual Fluctuations of the Tropical Pacific Wind Field and the Southern Oscillation. Monthly Weather Review, 110(6), 587–600. https://doi.org/10.1175/1520-0493(1982)110%3C0587:IFOTTP%3E2.0.CO;2

Persson A., (2006). Hadley's principle: understanding and misunderstanding the trade winds. History of Meteorology. 3. (online, last accessed 2022/01/18). http://meteohistory.org/2006historyofmeteorology3/2persson_hadley.pdf

Philander S., (1983). El Niño Southern Oscillation phenomena. Nature, 302, 295–301. https://doi.org/10.1038/302295a0

Pierson, W. J., & Marks, W. (1952). The power spectrum analysis of ocean-wave records. Eos, Transactions American Geophysical Union, 33(6), 834–844. https://doi.org/10.1029/TR033i006p00834

Portilla, J., Ocampo-Torres, F., & Monbaliu, J. (2009). Spectral partitioning and identification of wind sea and swell. Journal of Atmospheric and Oceanic Technology, 26(1), 107–122. https://doi.org/10.1175/2008JTECHO609.1

Portilla-Yandún, J., Cavaleri, L., & Van Vledder, G. P. (2015). Wave spectra partitioning and long term statistical distribution. Ocean Modelling, 96(Part 96), 148–160. https://doi.org/10.1016/j.ocemod.2015.06.008

Portilla-Yandún, J., & Cavaleri, L. (2016). On the specification of background errors for wave data assimilation systems. Journal of Geophysical Research: Oceans, 121, 209–223. https://doi.org/10.1002/2015JC011309

Portilla-Yandún, J., Salazar, A., Cavaleri, L., 2016. Climate patterns derived from ocean wave spectra. Geophys. Res. Lett. 43 (section 2), 1–8. http://doi.org/10.1002/2016GL071419

Portilla-Yandún, J. (2018). The global signature of ocean wave spectra. Geophysical Research Letters, 45, 267– 276. https://doi.org/10.1002/2017GL076431

Portilla-Yandún, J., Barbariol, F., Benetazzo, A., Cavaleri, L., 2019. On the statistical analysis of ocean wave directional spectra. Ocean Eng. 189, 106361. https://doi.org/10.1016/j.oceaneng.2019.106361

Ramage C., (1971), Monsoon Meteorology. Academic Press, New York, 296 pp. International geophysics series, V15, ISBN: 0125766505.

Reiter E., (1978). Long-Term Wind Variability in the Tropical Pacific, Its Possible Causes and Effects. Monthly Weather Review, 106(3), 324–330. https://doi.org/10.1175/1520-0493(1978)106%3C0324:LTWVIT%3E2.0.CO;2

Snodgrass, F., G. Groves, K. Hasselmann, G. Miller, W. Munk, and W. Powers (1966), Propagation of Ocean Swell across the Pacific, Philos. Trans. R. Soc. London, Ser. A, 259(1103), 431–497.

Trenberth, K. E., 1984: Signal versus noise in the Southern Oscillation. Mon. Wea. Rev.,112, 326–332. https://doi.org/10.1175/1520-0493(1984)112%3C0326:SVNITS%3E2.0.CO;2

Vesanto, J., Himberg, J., Alhoniemi, E., Parhankangas, J., (2000). SOM Toolbox for Matlab 5. Technical Report A57, vol. 2, p. 59 (0). http://www.cis.hut.fi/somtoolbox/package/papers/techrep.pdf

Wyrtki K., Meyers G., (1976). The Trade Wind Field Over the Pacific Ocean. Journal of Applied Meteorology, 15(7), 698–704. https://doi.org/10.1175/1520-0450(1976)015%3C0698:TTWFOT%3E2.0.CO;2

Young, I., and Holland, G. (1996). Atlas of the Oceans: Wind and Wave Climate. Cambridge: Pergamon. ISBN 978-0-08-042441-5.